Molecular Crystals and Liquid Crystals Science and Technology. Section A. Molecular Crystals and Liquid Crystals
Publication details, including instructions for authors and subscription information:
http://www.tandfonline.com/loi/gmcl19

Small Angle Light Scattering from Bipolar Nematic Droplets

J. Ding [a] & Y. Yang [a]
[a] Department of Macromolecular Science, Fudan University, Shanghai, 200433, China
Version of record first published: 23 Sep 2006.

To cite this article: J. Ding & Y. Yang (1994): Small Angle Light Scattering from Bipolar Nematic Droplets, Molecular Crystals and Liquid Crystals Science and Technology. Section A. Molecular Crystals and Liquid Crystals, 257:1, 63-87

To link to this article: http://dx.doi.org/10.1080/10587259408033765

Mol. Cryst. Liq. Cryst., 1994, Vol. 257, pp. 63–87
Reprints available directly from the publisher
Photocopying permitted by license only

Small Angle Light Scattering from Bipolar Nematic Droplets

J. DING and Y. YANG†

Department of Macromolecular Science, Fudan University, Shanghai 200433, China

(Received June 25, 1993; in final form February 3, 1994)

Theoretical and experimental studies are made of small angle light scattering (SALS) from the nematic droplets with a bipolar director configuration. Serial expressions for the scattered amplitudes from a single bipolar anisotropic sphere such as a bipolar nematic droplet are obtained using Rayleigh–Gans (RG) theory. Analytical solutions are also derived under reasonable approximations. All of the formulae are suitable for an arbitrary orientation of the droplet symmetry axis. Series of calculated Hv and Vv scattering patterns for the bipolar nematic droplets with typical orientations of droplet axes are presented. Some theoretical patterns have been confirmed in experiment with polymer dispersed liquid crystal (PDLC) films. As a result, SALS is proven useful to distinguish the director configurations of nematic droplets, and further to discriminate the orientations of the droplet axes. Moreover, the average size of the bipolar nematic droplets can be estimated by Hv scattering with the formulae given in this paper, and Vv scattering pattern can serve to evaluate the relative polarizabilities of PDLC films between anisotropic entities and isotropic mediums. Some inprecise interpretations for scattering photographs in literature are pointed out and clarified.

Keywords: Small angle light scattering, anisotropic sphere, bipolar director configuration, nematic droplet, polymer dispersed liquid crystal.

1. INTRODUCTION

Recently, the technique of polymer dispersed liquid crystal (PDLC) has attracted both theoretical and experimental physicists due to its prospective applications for large-area display.[1–9] A PDLC film is prepared by dispersing nematic droplets into a solid polymer matrix. According to Reference 5, there are basically three typical director configurations in nematic droplets called radial, bipolar and axial, as depicted schematically in Figure 1. The nematic droplets in the PDLC films have a typical radius of about 0.1–10 μm, which are in the range of small angle light scattering (SALS) studies. Hence, attention is focused on investigating SALS from nematic droplets.

Scattering from small particles is a classic physical problem in the last hundred years.[10–12] Most studies have been devoted to isotropic objects.[10–12] There are few analytical solutions for the light scattering from small, optically anisotropic objects. In 1960, using the model method and the Rayleigh–Gans (RG) theory, Stein *et al.*[13] made an analytical interpretation for the scattered amplitudes from a kind of anisotropic spheres, polymer spherulites, which laid a foundation to explore the structure of spherulite by SALS and resulted in great success.[13–15] SALS from nematic droplets has

† To whom the correspondance should be addressed.

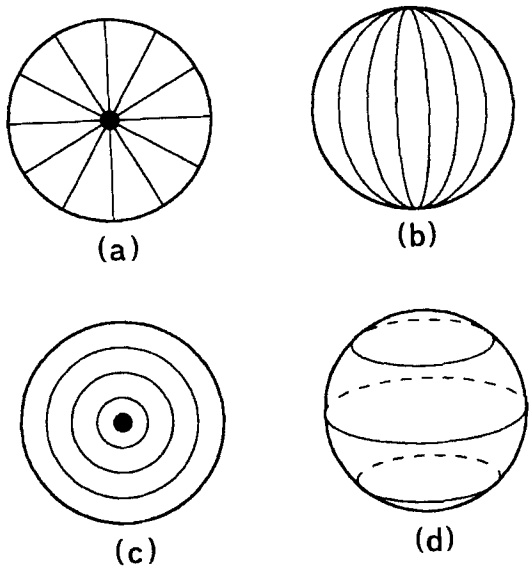

FIGURE 1 Three typical director configurations of nematic droplets: a) radial; b) bipolar; c) and d) axial.

been treated by some approximation approaches: RG approximation for relatively small nematic droplets,[16] the anomalous diffraction (AD) approximation for large droplets,[17] and the geometrical-optics approximation for very large objects.[18] Some comparison between scattering data and theory for nematic droplets has been performed by Whitehead *et al.*[19] In the way of Stein,[13] we obtain the analytical interpretations for SALS from typical nematic droplets. What is more, the analytical formulae given in this paper are suitable for an arbitrary orientation of the droplet axis.

SALS from the radial nematic droplets is optically the same as that of polymer spherulites, which has been studied previously.[13,14] Bipolar and axial nematic droplets are more complex because the symmetries of optical constants do not coincide with those of droplet shapes. The theoretical studies on the axial droplets has been published in another paper.[20] Explored mainly in this paper is theoretical and experimental studies on the nematic droplets with the bipolar director configuration. The analytical expression for SALS from the bipolar nematic droplet in an isotropic matrix is presented. Series of corresponding calculated scattering patterns are given, and are further confirmed in experiment. Some applications of SALS in the field of nematic droplets and PDLC are discussed and some confusions in literature are clarified.

2. THEORY OF SALS FROM BIPOLAR NEMATIC DROPLETS

2.1. Model of the Bipolar Director Field

In order to describe the bipolar director alignment, an elliptic model is introduced. The mass centers of nematic molecules are reasonably assumed to be arranged along series of ellipsoids, layer by layer. The ellipsoid shown in Figure 2 has a long principal axis with length of $2R$ and two short principal axes with length of $2R'$. The ratio of the short

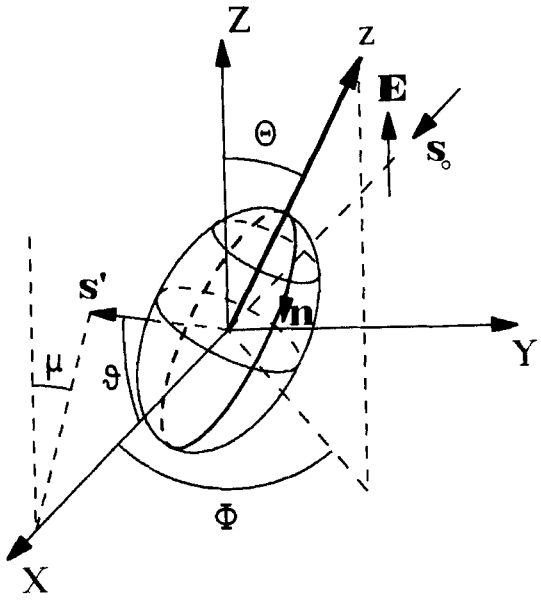

FIGURE 2 The coordinate systems for describing SALS from the bipolar nematic droplet. (X, Y, Z) is the lab frame while (x, y, z) is the droplet axis frame with the z-axis located at the principal symmetry axis of the droplet, the orientation of which is described by Θ and Φ. The s_0, **E** and **s'** are the unit vectors along the directions of incidence, polarization and scattering, respectively. The scattered beam is described by ϑ and μ. **n** refers to the local optical director in the bipolar nematic droplet.

and long axes is defined as f, that is, $f = R'/R$, where $f \in (0, 1]$. For later convenience, we let $f = \sin\beta$, where $\beta \in (0, \pi/2]$. Then the vector distance r is expressed by

$$r = R\,(\sin\beta\,\sin\alpha\,\cos\varphi\,\mathbf{i} + \sin\beta\,\sin\alpha\,\sin\varphi\mathbf{j} + \cos\alpha\mathbf{k}) \tag{1}$$

where **i**, **j** and **k** are the basic vectors of the droplet axis frame; α and φ are two angles in the ordinary polar coordinate system corresponding to this frame. Supposing the local nematic director in the bipolar droplet is tangential with the elliptic line, the bipolar director under the elliptic model can be expressed as

$$\mathbf{n} = \frac{\partial\mathbf{r}/\partial\alpha}{|\partial\mathbf{r}/\partial\alpha|} = \frac{1}{\sqrt{1-(\cos\beta\,\cos\alpha)^2}}(\sin\beta\,\cos\alpha\,\cos\varphi\mathbf{i} + \sin\beta\,\cos\alpha\,\sin\varphi\mathbf{j} - \sin\alpha\mathbf{k}) \tag{2}$$

It is worthy of noting that the changes of local order parameters within droplet and at the surface are not taken into considerations and that the director field in a bipolar nematic droplet may be different slightly from that described by the elliptic model. In fact, approximating the bipolar director field by segments of circles of appropriate radius[8] will be better than using such ellipses, because the director field around each

surface defect resembles the one of the hedgehog defects. A corresponding model, the bispheric model is therefore employed to describe the bipolar director field and to test the elliptic model by one of the authors.[25] (Unfortunately, the bispheric model can not lead to an analytical solution for SALS, so we will not describe it in details.) The volumes where both models deviate from the real simulation are relatively small and thus may not contribute much to the scattering. Our calculations also show that the scattering patterns under these two models are in accord with each other satisfactorily. Hence, we think that it is very useful to introduce the elliptic model, because such an ideal continuum model characterizes the basic structure of the bipolar droplet and brings about convenience to express the bipolar director field and corresponding SALS formulae analytically.

2.2. Serial Expressions for the Scattered Amplitudes from a Single Bipolar Nematic Droplet

According to RG scattering theory, the SALS from an isotropic spheres immersed in isotropic mediums can be interpreted by making use of the model method. A single droplet is dealt with at first. The scattered amplitude can, in the far field regime, be expressed in terms of the conventional integral;[10–13]

$$E_s = K \int (\mathbf{M}\cdot\mathbf{O}) e^{-ikr\cdot s} d\Omega \tag{3}$$

where K is a constant; $\mathbf{M}$ is the dipole moment induced by the incident electric field in the volume element at the vector distance $\mathbf{r}$; $\mathbf{O}$ is a unit vector parallel to the direction of analyzer; k is the wave number, $2\pi/\lambda_m$, where λ_m is the wavelength within medium. The integral above has been successfully employed to deal with light scattering from a polymer spherulite by Stein *et al.*[13] It reflects, in fact, the physical basis of the RG scattering, although Stein *et al.* failed to indicate this point in Reference 13. For RG approximation to be valid, two conditions must be satisfied,

$$|n_{LC}/n_m - 1| \ll 1 \tag{4}$$

$$2kR|n_{LC}/n_m - 1| \ll 1 \tag{5}$$

where n_{LC} is the effective refractive index of liquid crystal (LC) and n_m, the refractive index of the isotropic medium. The first condition may be interpreted as the requirement that the incident wave is not appreciably "reflected" at the particle-medium interface and the object is, therefore, optically "soft". Nematic droplets in PDLC films can be assumed to be optically soft, which is usually justified.[16–18] The second condition may be interpreted as the requirement that the incident wave does not undergo appreciable change of phase or amplitude after it enters the particle and the field inside the particle is, therefore, approximated by the incident field. Hence, RG theory is suitable for relatively small particles although they may be larger than in the Rayleigh theory. It was suggested by Zumer *et al.*[16] that for a kind of PDLC films they studied, the droplet diameter should not exceed 0.3 μm if a reasonably good description

is desired. We would like to point out that the suitable range of applicability of RG theory for droplet sizes depends on the degree of the optical softness of the object. If the difference between n_{LC} and n_m is smaller than 0.2, the suitable range may be larger than 0.3 μm and corresponding scattered light may, therefore, be concentrated within smaller scattering angles, which will bring about convenience for the experimental observation of scattering patterns. We would further note that actually, it is an anisotropic sphere with the bipolar director configuration surrounded by an isotropic medium that is dealt with in this paper. Nematic droplets in PDLC films are only taken as an example because of their prospective applications.

The scattering geometry for a bipolar nematic droplet is defined as in Figure 2, where the (x, y, z) coordinate system is the droplet axis frame with the z-axis located at the droplet symmetry axis, whereas (X, Y, Z) coordinate system is the lab frame which is determined by the directions of light incidence and polarization. Θ and Φ are the nutation angle and precession angle respectively. Since the bipolar droplet has cylindrical symmetry, the y-axis can be confined in XOY plane. The rotation angle is therefore fixed at zero. The incident and scattered beams are denoted by the unit vectors $\mathbf{s}_0$ and $\mathbf{s}'$ respectively, then the propagation vector $\mathbf{s}$ can be written as

$$\mathbf{s} = \mathbf{s}_0 - \mathbf{s}' = 2\sin\frac{\vartheta}{2}\left(\sin\frac{\vartheta}{2}\mathbf{I} - \cos\frac{\vartheta}{2}\sin\mu\mathbf{J} - \cos\frac{\vartheta}{2}\cos\mu\mathbf{K}\right) \tag{6}$$

where $\mathbf{I}$, $\mathbf{J}$ and $\mathbf{K}$ are the basic vectors of the lab frame; ϑ and μ are the scattering angle and azimuthal angle respectively, as defined as in Figure 2.

After transforming $\mathbf{s}$ into the droplet axis frame, we can get

$$k\mathbf{r}\cdot\mathbf{s} = U(s_1 \sin\beta \sin\alpha \cos\varphi + s_2 \sin\beta \sin\alpha \sin\varphi + s_3 \cos\alpha) \tag{7}$$

where

$$U = 2kR \sin\frac{\vartheta}{2} = \frac{4\pi R}{\lambda_m}\sin\frac{\vartheta}{2} \tag{8}$$

and

$$s_1 = \sin\frac{\vartheta}{2}\cos\Theta\cos\Phi - \cos\frac{\vartheta}{2}\sin\mu\cos\Theta\sin\Phi + \cos\frac{\vartheta}{2}\cos\mu\sin\Theta \tag{9.1}$$

$$s_2 = -\sin\frac{\vartheta}{2}\sin\Phi - \cos\frac{\vartheta}{2}\sin\mu\cos\Phi \tag{9.2}$$

$$s_3 = \sin\frac{\vartheta}{2}\sin\Theta\cos\Phi - \cos\frac{\vartheta}{2}\sin\mu\sin\Theta\sin\Phi - \cos\frac{\vartheta}{2}\cos\mu\cos\Theta \tag{9.3}$$

The polarizability of nematic molecules is of an uniaxial symmetry, the vector $\mathbf{M}$ can, therefore, be separated into two parts, parallel and perpendicular to the director, then we have

$$\mathbf{M} = \mathbf{M}_{\parallel} + \mathbf{M}_{\perp} = (\alpha_{\parallel} - \alpha_s)(\mathbf{E}\cdot\mathbf{n})\mathbf{n} + (\alpha_{\perp} - \alpha_s)[\mathbf{E} - (\mathbf{E}\cdot\mathbf{n})\mathbf{n}] \tag{10}$$

where **n** is the director, $\alpha_{\parallel}$ and $\alpha_{\perp}$ are the polarizabilities parallel and perpendicular to the director respectively, and α_s is the polarizability of the isotropic medium, **E** is the vector of polarized incident electric field with $\mathbf{E} = E_0 \mathbf{K}$.

In this paper, *Hv* and *Vv* scattering from bipolar nematic droplets are investigated. As is well known, *Hv* scattering refers to the scatering with analyzer perpendicular to the polarization of the incident light, i.e., $\mathbf{O} = \mathbf{J}$, while *Vv* scattering refers to the scattering with analyzer parallel to the polarization of the incident light, i.e., $\mathbf{O} = \mathbf{K}$. Then, we get

$$(\mathbf{M}\cdot\mathbf{O})_{Hv} = \frac{-\alpha_{12}E_0}{1-(\cos\beta\cos\alpha)^2}(A_1 \sin^2\beta\cos^2\alpha\cos^2\varphi + A_2 \sin^2\beta\cos^2\alpha\sin\varphi\cos\varphi + A_3 \sin\beta\sin\alpha\cos\alpha\cos\varphi + A_4 \sin\beta\sin\alpha\cos\alpha\sin\varphi + A_5 \sin^2\alpha) \quad (11)$$

$$(\mathbf{M}\cdot\mathbf{O})_{Vv} = \alpha_{20}E_0 + \frac{\alpha_{12}E_0}{1-(\cos\beta\cos\alpha)^2}(B_1 \sin^2\beta\cos^2\alpha\cos^2\varphi + B_2 \sin\beta\sin\alpha\cos\alpha\cos\varphi + B_3 \sin^2\alpha) \quad (12)$$

where

$$\alpha_{12} = \alpha_{\parallel} - \alpha_{\perp} \quad (13)$$

$$\alpha_{20} = \alpha_{\perp} - \alpha_s \quad (14)$$

and A_i and B_i are defined as follows:

$$A_1 = \sin\Theta\cos\Theta\sin\Phi \quad (15.1)$$

$$A_2 = \sin\Theta\cos\Phi \quad (15.2)$$

$$A_3 = \sin\Theta(\cos^2\Theta - \sin^2\Theta) \quad (15.3)$$

$$A_4 = \cos\Theta\cos\Phi \quad (15.4)$$

$$A_5 = -A_1 \quad (15.5)$$

and

$$B_1 = \sin^2\Theta \quad (16.1)$$

$$B_2 = 2\sin\Theta\cos\Theta \quad (16.2)$$

$$B_3 = \cos^2\Theta \quad (16.3)$$

After substituting Equations (7), (11) and (12) into Equation (3) and completing the integration (for the details, c.f., Appendix A), we finally obtain, in series, the exact solutions for *Hv* and *Vv* scattered amplitudes from a single bipolar anisotropic sphere such as a bipolar nematic droplet under RG approximation.

Our results are

$$E(Hv) = -3KE_0 V \alpha_{12} \sum_{m=0}^{\infty} \sum_{n=0}^{\infty} \sum_{k=0}^{n} C_{mnk} P_{mnk} \tag{17}$$

$$E(Vv) = 3KE_0 V \left(\alpha_{20} \frac{\sin U - U\cos U}{U^3} + \alpha_{12} \sum_{m=0}^{\infty} \sum_{n=0}^{\infty} \sum_{k=0}^{n} C_{mnk} Q_{mnk} \right) \tag{18}$$

where

$$C_{mnk} = 2(-1)^n U^{2n} s_3^{2k} (1 - s_3^2)^{n-k} \frac{m!(n+m+2)!(2k+2m)!(n-k+1)}{(2n+2m+5)!(n+m-k+2)!(k+m)!(2k+1)!} \tag{19}$$

and

$$\begin{aligned} P_{mnk} = {} & A_1 (2k+2m+1)(2k+1)\left[1 + \frac{2(n-k)s_1^2}{1-s_3^2}\right] \\ & + A_2 2(2k+2m+1)(n-k)(2k+1)\frac{s_1 s_2}{1-s_3^2} \\ & + A_3 4(2k+2m+1)(n-k)(n+m-k+2)\frac{s_1 s_3}{1-s_3^2} \\ & + A_4 4(2k+2m+1)(n-k)(n+m-k+2)\frac{s_2 s_3}{1-s_3^2} \\ & + A_5 4(n-k+2)(n+m-k+2)(2k+1) \end{aligned} \tag{20}$$

$$\begin{aligned} Q_{mnk} = {} & B_1 (2k+2m+1)(2k+1)\left[1 + \frac{2(n-k)s_1^2}{1-s_3^2}\right] \\ & + B_2 4(2k+2m+1)(n-k)(n+m-k+2)\frac{s_1 s_3}{1-s_3^2} \\ & + B_3 4(n-k+2)(n-m-k+2)(2k+1) \end{aligned} \tag{21}$$

It is worthy of emphasizing that the formulae are suitable for any orientation of the droplet axis. When α_{12} equals zero, i.e., $\alpha_{\parallel} = \alpha_{\perp} = \alpha$, the formulae are reasonably reduced to those describing SALS from an isotropic sphere under RG approximation:

$$E(Hv) = 0 \tag{22}$$

$$E(Vv) = KE_0 V \frac{3}{U^3}(\alpha - \alpha_s)(\sin U - U\cos U) \tag{23}$$

It should be complemented that in principle, Hv scattering from an isotropic sphere can occur.[11] However, Champion *et al.*[21] declared that even within the RG approximation, Hv scattering from an isotropic sphere might be measured, and Meeten[22] did

observe Hv scattering from "micron–diameter isotropic and spherical polymer latex". We would like to argue that there is no measurable small angle light scattering from an isotropic sphere when RG theory is applicable. The extra terms in Equations (23) and (24) in Reference 21 can be neglected if the entity is optically soft and observed within small scattering angles (these two conditions have, in fact, been introduced by them). We also doubt that the latex can be regarded as a completely isotropic sphere, because the latex is coated by a lyotropic polymeric LC surface. Although this anisotropic layer is thin, corresponding Hv scattering might not be neglected when the main body of latex is isotropic.

2.3. Analytical Interpretations under Approximations

Analytical formulae always bring about convenience for calculation. However, the analytical expressions for SALS from particles are scarce. Fortunately, calculations in computer reveal that the series given above converge rapidly, especially for the index m. This can be shown by comparison of the calculated scattering patterns for the bipolar droplet with a typical orientation of the droplet axis (see Figure 3). Figure 3 indicates that even under zeroth order approximation ($m = 0$), the output already embodies the

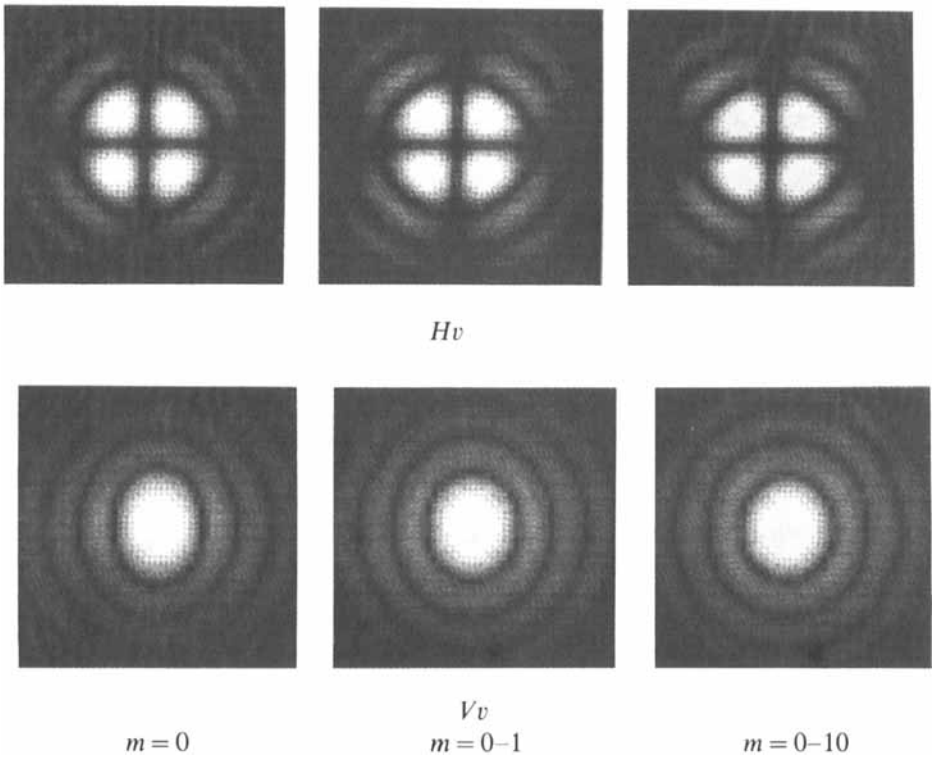

FIGURE 3 Theoretical Hv and Vv scattering patterns for the bipolar nematic droplet with $\Theta = 0°$ and $\Phi = 0°$ calculated under zeroth, first and tenth order approximations. For Vv scattering, $\alpha_{12} = 1$ and $\alpha_{20} = 0$. ($\lambda_m = 0.6328\,\mu m$; $R = 10\,\mu m$; area shown: $8° \times 8°$ for ϑ).

main characteristics of the final scattering pattern, and the first order approximation ($m = 0 - 1$) can be accurate enough to deal with the light scattering in small angle from the bipolar nematic droplet. This result has been proven justified both for Hv and Vv scatterings in the case of other complicated orientations of the droplet axis.

By setting $m = 0$ or $m = 0 - 1$ and summing up the indices n and k, we obtain the analytical interpretations for SALS from a single bipolar nematic droplet under the zeroth and first order approximations respectively. The theoretical results under the first order approximation are given as follows:

$$\begin{aligned} E(Hv) = 3KE_0V\frac{\alpha_{12}}{(1-s^2)^4U^7}[&H_1U^5\cos U + H_2U^4\sin U + H_3U^3\cos U \\ &+ H_4U^2\sin U + H_5U\cos U + H_6\sin U \\ &+ H_7U^3\cos(s_3U) + H_8U^2\sin(s_3U) + H_9U\cos(s_3U)] \end{aligned} \tag{24}$$

where

$$H_1 = (1-s_3^2)^3[(A_1s_1 + A_2s_2)s_1s_3^2 + (A_3s_1 + A_4s_2)s_3(1-s_3^2) + A_5(1-s_3^2)^2] \tag{25.1}$$

$$\begin{aligned} H_2 = (1-s_3^2)[&A_1s_3^2(1-s_3^2)^2 + (A_1s_1 + A_2s_2)s_1(1 - 12s_3^2 + 19s_3^4 - 8s_3^6) \\ &+ (A_3s_1 + A_4s_2)2s_3(-3 + 4s_3^2)(1-s_3^2)^2 + A_5 2(1-2s_3^2)(1-s_3^2)^3] \end{aligned} \tag{25.2}$$

$$\begin{aligned} H_3 = &A_1(-1 + 8s_3^2 - 18s_3^4 + 16s_3^6 - 5s_3^8) \\ &+ (A_1s_1 + A_2s_2)s_1(7 - 64s_3^2 + 150s_3^4 - 128s_3^6 + 35s_3^8) \\ &+ (A_3s_1 + A_4s_2)s_3(1-s_3^2)(-21 + 85s_3^2 - 99s_3^4 + 35s_3^6) \\ &+ A_5 5(-1 + 7s_3^2)(1-s_3^2)^4 \end{aligned} \tag{25.3}$$

$$\begin{aligned} H_4 = &A_1(3 - 24s_3^2 + 62s_3^4 - 56s_3^6 + 15s_3^8) \\ &+ (A_1s_1 + A_2s_2)3s_1(-7 + 80s_3^2 - 190s_3^4 + 136s_3^6 - 35s_3^8) \\ &+ (A_3s_1 + A_4s_2)s_3(1-s_3^2)(75 - 295s_3^2 + 309s_3^4 - 105s_3^6) \\ &+ A_5 15(1 - 7s_3^2)(1 - s_3^2)^4 \end{aligned} \tag{25.4}$$

$$H_5 = -(H_6 + H_9) \tag{25.5}$$

$$H_6 = -30(1-s_3^2)^4[A_1(1 - 7s_1^2) - A_2 7s_1s_2 + A_3 7s_1s_3 + A_4 7s_2s_3 + A_5(1 - 7s_3^2)] \tag{25.6}$$

$$H_7 = 4(1-s_3^2)[A_1(-1+s_3^2+4s_1^2)+A_2 4s_1 s_2] \tag{25.7}$$

$$H_8 = 8[A_1 s_3(-1+s_3^2+6s_1^2)+A_2 6s_1 s_2 s_3+(A_3 s_1+A_4 s_2)2(1-s_3^2)] \tag{25.8}$$

$$H_9 = 24[A_1(1-s_3^2-6s_1^2)-A_2 6s_1 s_2] \tag{25.9}$$

$$\begin{aligned} E(Vv) = 3KE_0 V\Big\{ & \alpha_{20}\frac{\sin U - U\cos U}{U^3} - \frac{\alpha_{12}}{(1-s_3^2)^4 \mathbf{U}^7} \\ & \times [V_1 U^5 \cos U + V_2 U^4 \sin U + V_3 U^3 \cos U \\ & + V_4 U^2 \sin U + V_5 U \cos U + V_6 \sin U \\ & + V_7 U^3 \cos(s_3 U) + V_8 U^2 \sin(s_3 U) + V_9 U \cos(s_3 U)]\Big\} \end{aligned} \tag{26}$$

where

$$V_1 = (1-s_3^2)^3[B_1 s_1^2 s_3^2 + B_2 s_1 s_3(1-s_3^2) + B_3(1-s_3^2)^2] \tag{27.1}$$

$$\begin{aligned} V_2 = (1-s_3^2)[& B_1 s_3^2(1-s_3^2)^2 + B_1 s_1^2(1-12s_3^2+19s_3^4-8s_3^6) \\ & + B_2 2s_1 s_3(-3+4s_3^2)(1-s_3^2)^2 + B_3 2(1-2s_3^2)(1-s_3^2)^3] \end{aligned} \tag{27.2}$$

$$\begin{aligned} V_3 = B_1[& -1+8s_3^2-18s_3^4+16s_3^6-5s_3^8 \\ & + s_1^2(7-64s_3^2+150s_3^4-128s_3^6+35s_3^8)] \\ & + B_2 s_1 s_3(1-s_3^2)(-21+85s_3^2-99s_3^4+35s_3^6) \\ & + B_3 5(-1+7s_3^2)(1-s_3^2)^4 \end{aligned} \tag{27.3}$$

$$\begin{aligned} V_4 = B_1[& 3-24s_3^2+62s_3^4-56s_3^6+15s_3^8 \\ & + s_1^2(-21+240s_3^2-570s_3^4+408s_3^6-105s_3^8)] \\ & + B_2 s_1 s_3(1-s_3^2)(75-295s_3^2+309s_3^4-105s_3^6) \\ & + B_3 15(1-7s_3^2)(1-s_3^2)^4 \end{aligned} \tag{27.4}$$

$$V_5 = -(V_6+V_9) \tag{27.5}$$

$$V_6 = -30(1-s_3^2)^4[B_1(1-7s_1^2)+B_2 7s_1 s_3 + B_3(1-7s_3^2)] \tag{27.6}$$

$$V_7 = B_1 4(1-s_3^2)(-1+s_3^2+4s_1^2) \tag{27.7}$$

$$V_8 = 8[B_1 s_3(-1+s_3^2+6s_1^2)+B_2 2s_1(1-s_3^2)] \tag{27.8}$$

$$V_9 = B_1 24(1-s_3^2-6s_1^2) \tag{27.9}$$

All the theoretical scattering patterns for bipolar nematic droplets given in the next section are calculated with the formulae under the first order approximation. For comparison, the analytical interpretation under the zeroth order approximation are presented in Appendix B.

3. SERIES OF THEORETICAL SCATTERING PATTERNS

3.1. Scattering Patterns for Seven Typical Orientations of a Bipolar Nematic Droplet

Different from the radial sphere, the bipolar droplet has a cylinderic symmetry axis, therefore the orientation of the droplet axis must be taken into considerations. Attention is paid to seven typical orientations. All the expressions for SALS from the bipolar droplet in this paper have no limitation to the orientation of the droplet axis at all. Hence, the analytical expression for the scattered amplitude from a single bipolar droplet with any specific orientation can be written down readily. In order to see the variabilities of the scattering patterns for the bipolar nematic droplets and to bring about convenience for later consulting, a series of Hv scattering patterns for the bipolar nematic droplet have been calculated and are shown in Figure 4, while Vv scattering patterns, in Figure 5. For each pattern, corresponding orientational angles, namely, Θ and Φ, are marked below. The given patterns are calculated for the first order approximation. It is necessary to note that for each pattern, the zeroth order approximation and the first order approximation are checked carefully and proven both effective.

Vv scatterings such as leaf-orientations of scattering patterns are sensitive to the relative polarizabilities between anisotropic entities and isotropic mediums very much.[13,14] Typical relative polarizabilities are considered with four groups of proportions of α_{12} and α_{20}: (0, 1),(1, 0),(1, 1) and (1, $-$1). The case (0, 1) refers to an isotropic sphere and is, therefore, not shown in Figure 5. The Vv scattering with any combination of $\alpha_{\parallel}, \alpha_{\perp}$ and α_s, in our opinion, results from the sum of two kinds of scatterings in the amplitude way: one is the isotropic type in the case of (0, 1), the other is the so called anisotropic type in the case of (1, 0), which is contributed only by the anisotropic contrast factor α_{12}. This can be seen both from Equations (18) and (26) and from scattering patterns in Figure 5. Hence, it is the proportion of α_{12} and α_{20} that determines the final Vv scattering pattern for a nematic droplet with a definite director configuration and a definite orientation of the droplet axis. Therefore, the scattering pattern with (α_{12}, α_{20}) taking the proportion of (1, 0) is a key to describing a series of Vv patterns with different relative polarizabilities.

It should be noted that the results obtained from a single nematic droplet cannot be extended to that from a PDLC film in principle, because the PDLC film is a system with multiple particles. Just as Zumer *et al.*[7] has indicated, the spatial distribution of the scattering objects influences the transmitted light through two effects, interference and multiple scattering. Nevertheless, these two effects are neglected tentatively in present paper, since we pay attention not to scattered intensities quantitatively, but to the main characteristics of scattering patterns qualitatively. Similar to the case of SALS from

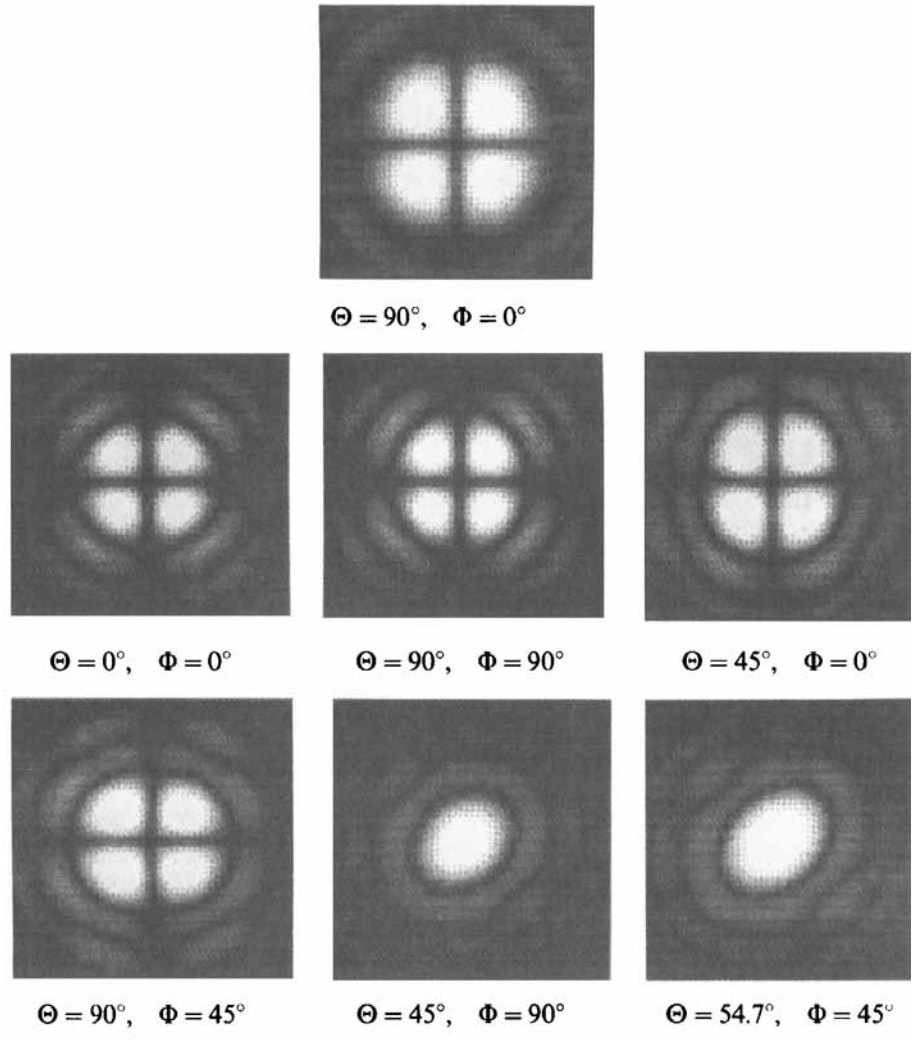

FIGURE 4 Calculated Hv scattering patterns for the bipolar nematic droplet with seven typical orientations of the droplet axis. The orientational angles Θ and Φ are noted below each corresponding scattering pattern. Other pertinent parameters are the same as those in Figure 3.

spherulites,[13–15] the scattering pattern for a single bipolar nematic droplet with a typical orientation of the droplet axis may, in our opinion, reflect the characteristic pattern for multiple bipolar droplets with the same orientation and the same size, provided that the scatterings from different particles are incoherent. This may be usually justified in the case of PDLC because the positions of nematic droplets in PDLC films are usually distributed randomly in the illuminated volume and the numbers and orientations of scattering sites are difficult to fluctuate in such a kind of solid films. To neglect multiple scattering is also not a severe limitation because it does

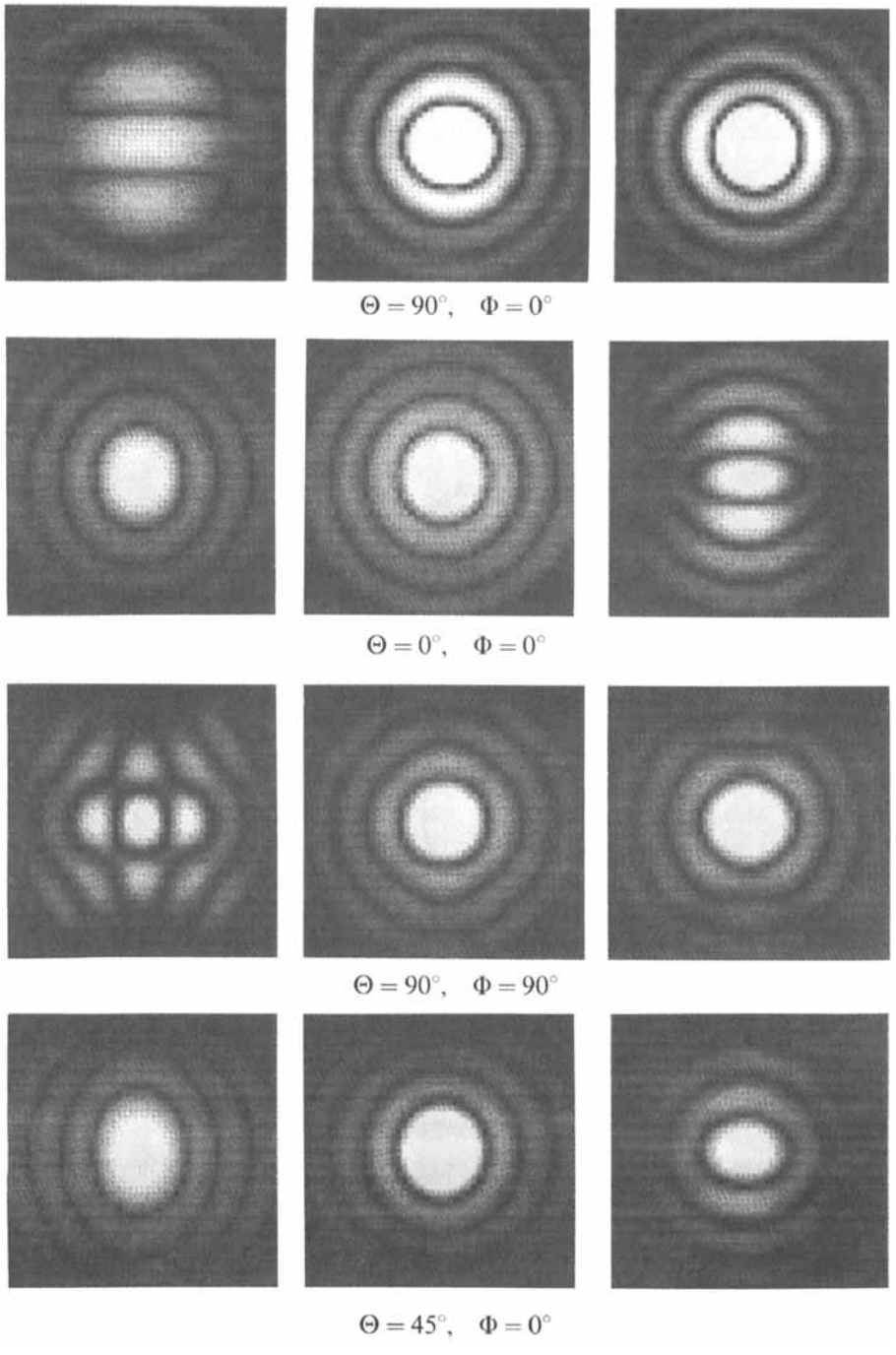

FIGURE 5 Calculated Vv scattering patterns for the bipolar nematic droplet with seven typical orientations of the droplet axis under three kinds of relative polarizabilities (α_{12}, α_{20}). Other pertinent parameters are the same as those in Figure 3. (To be continued)

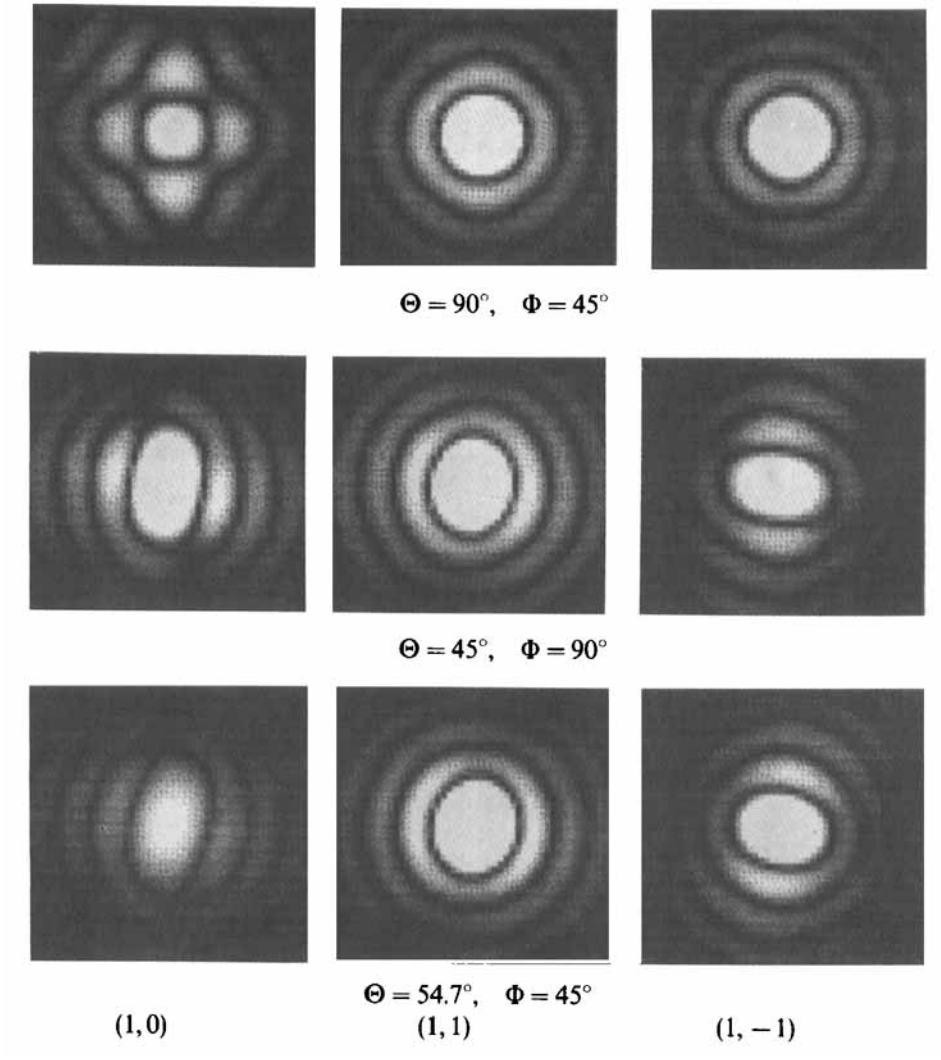

FIGURE 5 (*Continued*)

not predominently affect the distribution of the scattered light from the relatively thin, optically soft PDLC films.

3.2. Scattering Patterns for the Random Orientation of Bipolar Nematic Droplets

Droplet axes will be oriented randomly if no external field is imposed on PDLC films in sample preparation.[9] Neglecting interference effect and multiple scattering, we express, for simplicity, the total scattered intensity as the sum of the scattered intensities from all

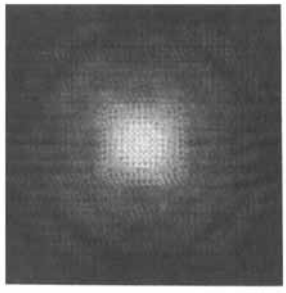

FIGURE 6 Calculated Hv scattering pattern for the bipolar nematic droplets with the random orientation of droplet axes. The pertinent parameters are the same as those in Figure 3.

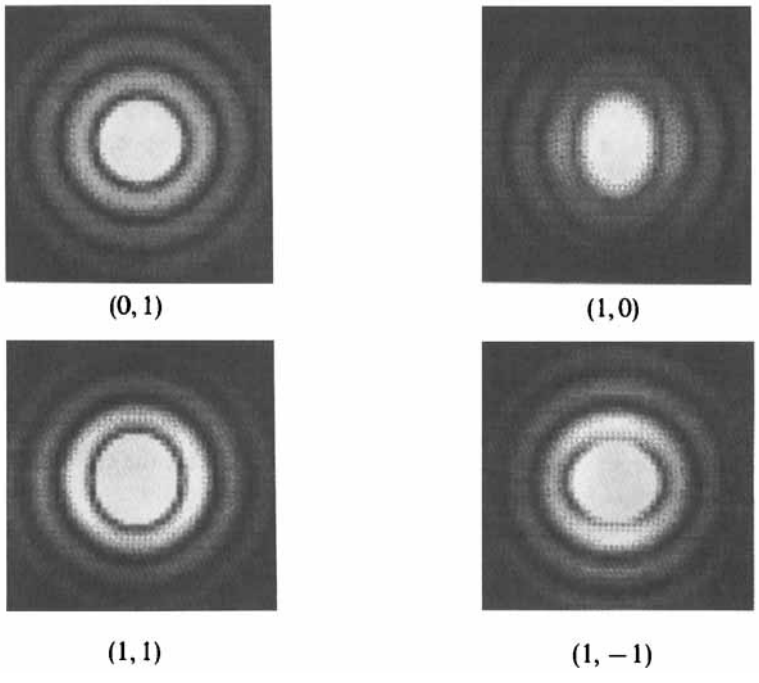

FIGURE 7 Calculated Vv scattering patterns for the bipolar nematic droplets with the random orientation of droplet axes under four groups of relative polarizabilities, $(\alpha_{12}, \alpha_{20})$. Here, the case (0, 1) represents Vv scattering from an isotropic sphere. Other pertinent parameters are the same as those in Figure 3.

nematic droplets with the same size but with various orientations of droplet axes.

$$I = \int_0^{2\pi} \int_0^{\pi} I(\Theta, \Phi) \sin\Theta \, d\Theta \, d\Phi \Big/ \int_0^{2\pi} \int_0^{\pi} \sin\Theta \, d\Theta \, d\Phi \tag{28}$$

In the following calculation, the integration was converted into summation:

$$I = \sum_{j=1}^{180/\Delta\Theta} \sum_{k=1}^{180/\Delta\Phi} I(\Theta_j, \Phi_k) \sin\Theta_j \Delta\Theta \Delta\Phi \Big/ \left[180 \sum_{j=1}^{180/\Delta\Theta} \sin\Theta_j \Delta\Theta \right] \tag{29}$$

It should be noted that such a treatment is not strict and is tentatively used by the authors to obtain some characteristics of scattering patterns instead of quantitative scattered intensities. Calculated results indicate that it is fine enough to take $\Delta\Theta = 10°$ and $\Delta\Phi = 18°$. The corresponding Hv and Vv scattering patterns are shown in Figures 6 and 7 respectively. For the sake of comparison, Vv scattering from an isotropic sphere, i.e., $\alpha_{12} = \alpha_{\parallel} - \alpha_{\perp} = 0$, is shown in the first pattern of Figure 7.

4. EXPERIMENT OF SALS FROM PDLC FILMS

The method of polymerization-induced phase separation[23,24] was used to prepare two kinds of samples, PMA-based PDLC and epoxy-based PDLC. The PMA-based PDLC film was made from the solution of a kind of low molecular nematic liquid crystal, E7 (BDH Ltd) dissolved in the mixture of methyl acrylate monomer and 1% of UV initiator, AIBN, in a 1:2 weight ratio. The solution was sandwiched between two glass plates with spacer about 40 μm. The sandwich was then exposed in UV made with radiation from a 200 W medium pressure mercury arc 30 cm away from the sandwich for 30 s. The phase separation took place with the polymerization of monomers into Poly(methyl acrylate) (PMA) and nematic droplets were hence formed. In preparation of epoxy-based PDLC, the nematic E7, epoxy resin (E-51) and amine curing agent (triethylenetetramine) were mixed thoroughly with the proportion 1:1:0.6 by weight, the mixer was also sandwiched between two glass plates with spacer about 40 μm. Then the film was cured at 70 °C for 2 hours and the epoxy-based PDLC resulted in phase separation. The refraction index of the liquid crystal has the principal values $n_e = 1.7$ and $n_0 = 1.5$ while the bulk epoxy resin has index $n_s = 1.5$. (Actual polymer index may increase to some degree with part of liquid crystals retained in the solid matrix and the condition of optical softness can therefore be satisfied better).

By means of polarized optical microscopy (POM), the authors have elucidated that the nematic droplets in the PMA-based PDLC and the epoxy-based PDLC have the radial and bipolar director configurations respectively, and the principal axes of bipolar droplets are oriented randomly.[9,25–27] Observed under a Leitz polarizing microscope, the droplet sizes of both samples are relatively uniform ($R \sim 5$ μm), and the difference is that all droplets in PMA-based PDLC have cross extinction while those in epoxy-based PDLC take various extinction patterns. Corresponding theoretical and experimental work have been or will be published elsewhere.[9,26,27]

SALS measurements were carried out on a home-built apparatus with He–Ne laser ($\lambda = 632.8$ nm) as the incident light source. The detailed description of the apparatus can be found in Reference 13. The Hv and Vv scattering photographs of the two samples are shown in Figures 8 and 9. For each photograph, the corresponding theoretical pattern is given.

It should be pointed out that one of the RG approximation conditions given in Equation (5) is not realized considering the large average radius of the nematic droplets and the refraction difference of E7, although each theoretical pattern in Figures 8 and 9 do be in good agreement with corresponding experimental one. Similar phenomenon can frequently be observed in the field of spherulites and is well known by polymer

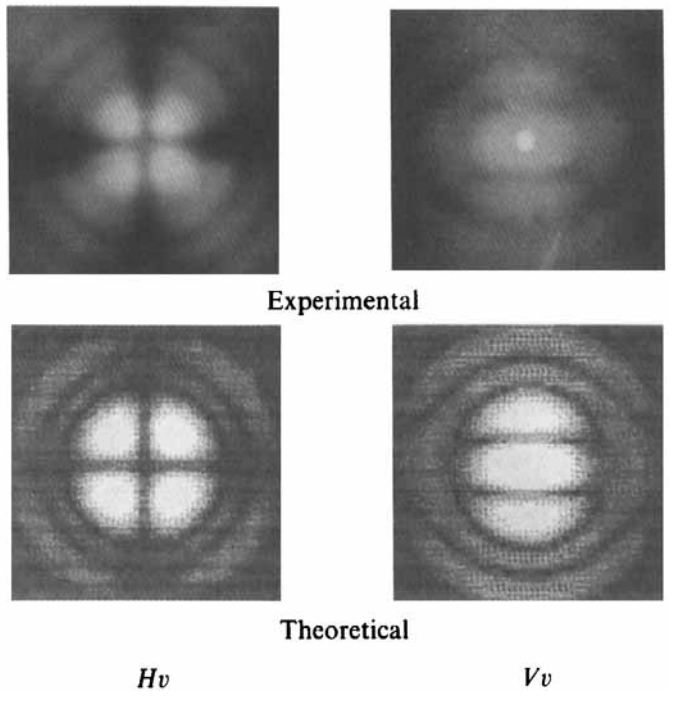

FIGURE 8 Experimental Hv and Vv laser scattering photographs of nematic droplets in the PMA-based PDLC-film and the corresponding theoretical scattering pattern on assumption of the radial director configuration, and furthermore for the Vv scattering, on assumption of relative polarizabilities similar to the case $\alpha_{12} = 1$ and $\alpha_{20} = 0$.

physicists.[13–15] It indicates that the characteristics of scattering patterns for anisotropic spheres within relatively small scattering angles are mainly determined by their internal director configurations and by the orientations of principal axes, and that they will not change seriously with sizes. It further implies that the applicable range of the series of scattering patterns given in this paper (not of the quantitative scattering intensities) might be wider than that restricted by Equation (5). But we should keep cautious in application of this extension, since RG theory is only qualitative for large droplets. Therefore, a precise comparison testing of the RG approximation with AD approximation[17] or even with Mie's scattering theory[10–12] is desired to determine in what region the RG theory is still appropriate for nematic droplets in PDLC films.

5. RESULTS AND DISCUSSIONS

In the past three sections, SALS from the bipolar nematic droplets has been investigated theoretically and partly confirmed experimentally. Three immediate applications of scattering patterns will be pointed out and discussed in this section.

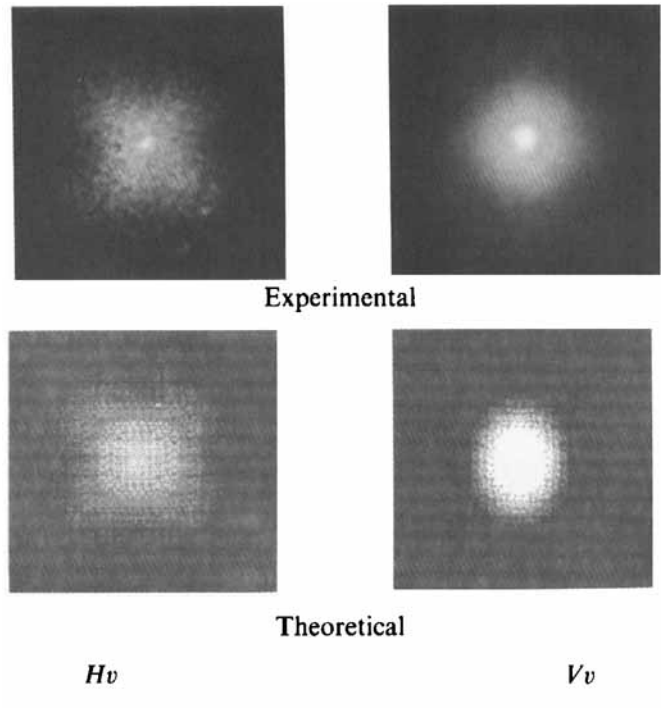

FIGURE 9 Experimental Hv and Vv laser scattering photographs of nematic droplets in the epoxy-based PDLC film and the corresponding theoretical scattering pattern on assumption of the bipolar director configuration with droplet axes oriented randomly, furthermore for the Vv scattering, on assumption of relative polarizabilities similar to the case $\alpha_{12} = 1$ and $\alpha_{20} = 0$.

5.1. Characterization of Director Configurations

The behaviour of the external field response of nematic droplets is effected by their director configurations. It is, therefore, very important to find out some methods to characterize the director configurations of nematic droplets. POM is one of good methods,[2,9,28] however, submicron nematic droplets can not be observed clearly under a polarizing microscope. ^{2}H-NMR may be useful in the case of submicron nematic droplets,[29] but it requires the use of deuterated LC samples. As has been indicated in the first section, nematic droplets in PDLC films have suitable sizes for SALS studies. The possibilities of determing the nematic director structure and the droplet size from experimental light scattering data have been pointed out by Zumer *et al.*[17] and will be confirmed in this section.

For comparison, the expressions for the scattered amplitudes from a single radial droplet or polymer spherulite[13,14] are rewritten as follows:

$$E(Hv) = KE_0 V \frac{3}{U^3} \alpha_{12} \cos^2 \frac{\vartheta}{2} \sin \mu \cos \mu (4 \sin U - U \cos U - 3\, SiU) \qquad (30)$$

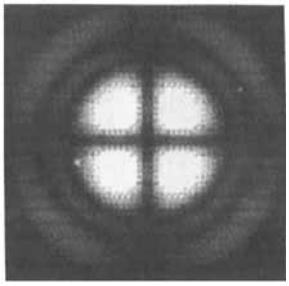

FIGURE 10 Calculated Hv scattering pattern for the radial nematic droplet. The pertinent parameters are the same as those in Figure 3.

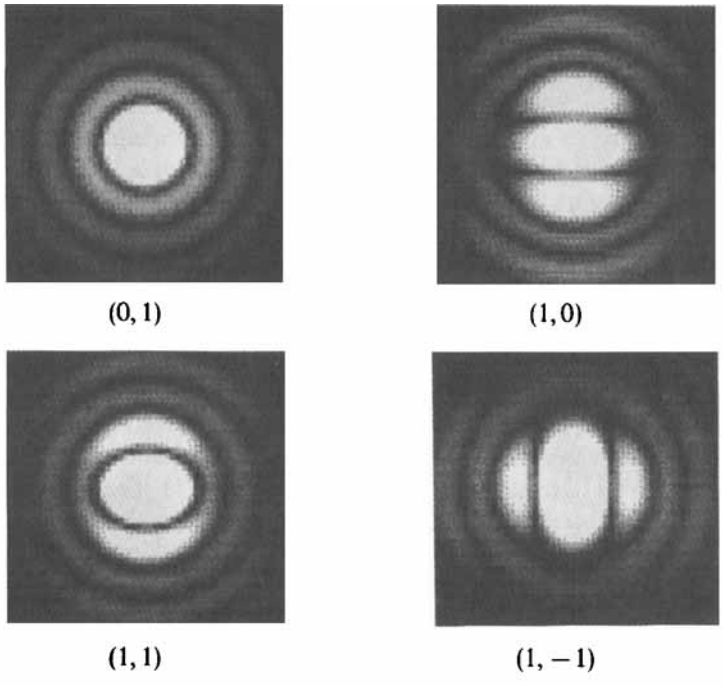

FIGURE 11 Calculated Vv scattering patterns for the radial nematic droplet under four groups of relative polarizabilities (α_{12}, α_{20}). Other pertinent parameters are the same as those in Figure 3.

$$E(Vv) = KE_0 V \frac{3}{U^3}\left\{\alpha_{20}(\sin U - U\cos U) + \alpha_{12}\left[SiU - \sin U + \cos^2\frac{\vartheta}{2}\cos^2\mu(4\sin U - U\cos U - 3\,SiU)\right]\right\} \tag{31}$$

where

$$SiU = \int_0^U \frac{\sin x}{x}dx \tag{32}$$

Corresponding Hv and Vv scattering patterns are shown in Figures 10 and and 11.

By comparing the scattering patterns given in Figures 4–7 and those in Figures 10 and 11, it is clear that the orientational dependence of the scattering patterns is peculiar to the bipolar nematic droplets and the difference among these scattering patterns is large enough to distinguish bipolar and radial director configurations. It also provides a method for estimating the orientation of the droplet axes for bipolar nematic droplets. Even the random orientation of bipolar nematic droplets can be discriminated from any uniform orientation.

It seems worthwhile to emphasize again that the scattering patterns for all kinds of nematic droplets except a radial one depend strongly on the orientation of droplet axes, and experimental scattering photographs should be interpreted with great caution. Margerum *et al.* reported a wonderful work on effects of off-state alignments in PDLC films.[24] But some analyses were not given in precise term, although their physical picture had no fundamental mistake. According to their observations that the laser scattering patterns for PDLC films were altered by the *E field polymerization induced phase separation formation*, they analysed that without a formation field, the scattering patterns were related to a tangential nematic droplet alignment, but with increased formation fields the scattering patterns showed increased evidence for the presence of a radial director alignment as well. Again, they attributed the decreased scattering from PDLC films formed in presence of transverse E fields to *field-induced radial director alignment*. (No scattering photograph was given in that paper). However, as we know, the radial director alignment is always related to a perpendicular boundary anchoring,[7,30] hence the tangential nematic droplet alignment can not be altered into a radial one with increased formation fields. The key is that the droplet axis may be oriented orthogonal to the sample plane with strong enough external fields, and corresponding scattering patterns are really difficult to discriminate with that from a radial droplet or a spherulite. In this case, most of nematic molecules within droplet are parallel or almost parallel with the incident light under normal incidence, therefore seems isotropic under this visual angle. Considering further the fact that the relation $\alpha_\perp \sim \alpha_s$ holds in PDLC films as usual, little contribution to the scattered light including Vv scattering is made by this part of nematic molecules in the sample with the formation field. That is the real reason that the scattering from PDLC films was decreased and such an experimental phenomenon has also been observed by us.[25] Actually, the term *field-induced radial director alignment* should be replaced by *field-induced orthogonal orientation of droplet axis*. The difficulties in explaining correctly the scattering photographs come mainly from lack of series of standard scattering patterns for nematic droplets. To resolve such a problem is just one of original motives for us to study SALS from nematic droplets and to present series of calculated scattering patterns.

5.2. Evaluation of Relative Polarizabilities

A composite system may have complicated relative polarizabilities among $\alpha_\parallel$, $\alpha_\perp$ and α_s, which is important in practical applications. For instance, the relation $\alpha_\perp \sim \alpha_s$ should hold in a PDLC film as usual, in order to obtain high contrast ratio by decreasing scattering in electric field *on* state. Vv scattering such as leaf-orientations of the

scattering patterns has been widely used to evaluate the relative polarizabilities between polymer spherulites and isotropic mediums.[13–15] It is also effective for nematic droplets according to theoretical and experimental results in this paper (Figures 5, 7–9 and 11). Although the evaluation is never quantitative, it does be helpful in practice for us to adjust the polarizabilities of the polymeric mediums in PDLC films.

5.3. Measurement of Droplet Sizes

The determination of the angular position of the scattering maximum in *Hv* scattering pattern affords a rapid means for measuring the average size of particles. It had been a traditional method in the case of polymer spherulites after the original work made by Stein *et al.*[13,14] The scattering maxima in *Hv* scattering pattern are located along the azimuthal angle $\mu = \pm 45°$ (see Figure 10), and corresponding ϑ_m can, therefore, be measured conveniently with the photographic light scattering technique, then the average radius of scattered spheres in the illuminated volume, $\bar{R}$, can be obtained because the wavelength of the scattered light within medium, λ_m, is known as usual and the value U at the scattered maximum, denoted as U_m, keeps basically constant within a certain range of sizes with the relation as follows:[13]

$$U_m = \frac{4\pi\bar{R}}{\lambda_m} \sin\frac{\vartheta_m}{2} = 4.09 \tag{33}$$

The formula for the radial nematic droplets is the same as that for ideal spherulites. Similarly, a series of ϑ_m under different droplet radii are calculated, from which the formulae to measure the sizes of the bipolar nematic droplets are obtained: $U_m = 4.68$ for the bipolar nematic droplet with (Θ, Φ) taking $(90°, 0°)$ and the scattering maxima are located along $\mu = \pm 45°$; $U_m = 3.86$, with (Θ, Φ) both taking $(0°, 0°)$ and $(90°, 90°)$ and in these cases, the azimuthal angles deviate slightly from $\pm 45°$ (see Figure 4). The degree of deviation is relevent to the average size of measured droplets. As the *Hv* scattering maximum for the bipolar droplets with the random orientation of droplet axes is located at the center of the scattering pattern, only the angles corresponding to high order scattering maxima such as the second and third order scattering maxima might be detected, with $U_m = 8.35$ and $U_m = 11.90$ respectively. High order scattering maxima in this case are located along $\mu = \pm 45°$ (see Figure 6). It has been found that the measured sizes by SALS agree satisfactorily with those by POM. For instance, the nematic droplets have an average radius $\bar{R} = 5.1 \pm 0.3$ μm according to the *Hv* pattern after the refraction at the glass-air surface has been revised, while by POM measurement, $\bar{R} = 4.9 \pm 0.7$ μm.

Equation (33) indicates that smaller nematic droplets give scattering patterns at larger angles. Nematic droplets smaller than 1 μm may be studied using a similar theoretical interpretation with photometric data, but too small nematic droplets might bring about difficulties for measurement although the light scattering technique can still be used in principle. It should also be noted that the constants given above are obtained according to the elliptic model. If the bipolar director deviates from that described by such an ideal model, the value of U_m may change to some degree.

Moreover, the exact value of U_m depends on particle sizes and size distributions as well as relative polarizabilities, as Champion *et al.* indicated.[21] It is also necessary to mension that the RA approximation will modify the position of interference maxima and minima, although it does not change the general structure of the pattern. For large droplets, this approach is only qualitative. Hence in many cases, the average size of nematic droplets can only be estimated. But anyway, SALS affords a good method to compare relatively the average sizes of particles in a series of samples.

6. CONCLUSIONS

From this study, we conclude that SALS can serve to distinguish the bipolar nematic droplet from a radial one, and further to discriminate the orientation of the bipolar droplet axis, which has been emphasized. The relative polarizabilities of PDLC films can also be evaluated by Vv scattering patterns, and the average size of droplets can be measured or estimated readily by Hv scattering. Since the electro-optic response mechanism of PDLC belongs to a scattering type, it is very important to calculate transmittance ratio by measurement or calculation of scattering intensities.[7,31-33] The treatment method and some results in this paper can be extended to deal with the total scattering effect of multiple nematic droplets. Finally, it should be noted that these results would also be suitable for the other anisotropic objects such as crystalline ones provided that they had the same director configurations as nematic droplets. The authors are confident that SALS will be a powerful technique to make extensive studies on anisotropic systems with various self-organized structures.

Acknowledgments

The authors gratefully acknowledge the financial support from NSF of China, FEYUT of SEDC and Chinese National Basic Project-Macromolecular Condensed State. We also thank Master Hongdong Zhang and Doctor Jianming Lu very much for their kind help with sample preparation of PDLC films.

References

1. J. L. Fergason, *SID (Society for Information Dislay) Ins. Symp. Dig. Tech. Papers*, **16**, 68 (1985).
2. P. S. Drzaic, *J. Appl. Phys.*, **60**, 2142 (1986).
3. J. W. Doane, N. A. Vaz, B. G. Wu and S. Zumer, *Appl. Phys. Lett.*, **48**, 269 (1986).
4. J. W. Doane, G. Chidichimo and N. A. Vaz, US Patent **4**, 688, 900 (1987).
5. P. S. Drzaic, *Mol. Cryst. Liq. Cryst.*, **154**, 289 (1988).
6. J. L. West, *Mol. Cryst. Liq. Cryst.*, **157**, 427 (1988).
7. S. Zumer, A. Golemme and J. W. Doane, *J. Opt. Soc. Am. A.*, **6**, 403 (1989).
8. J. H. Erdman, S. Zumer and J. W. Doane, *Phys. Rev. Lett.*, **64**, 1907 (1990).
9. J. Ding and Y. Yang, *Jpn. J. Appl. Phys.*, **31**, 2837 (1992).
10. M. Kerker, *The Scattering of Light and Other Electromagnetic Radiation* (Academic, New York, 1969).
11. H. C. Van de Hulst, *Light Scattering by Small Particles* (Wiley, New York, 1957).
12. C. F. Bohren and D. R. Hoffman, *Absorption and Scattering of Light by Small Particles* (Wiley, New York, 1983).
13. R. S. Stein and M. B. Rhodes, *J. Appl. Phys.*, **31**, 1873 (1960).
14. R. J. Samules, *J. Polym. Sci. A.*, **2**, 2163 (1971).
15. R. J. Samules, *Structured Polymer Properties* (John Wiley and Sons, Inc., New York, 1974).
16. S. Zumer and J. W. Doane, *Phys. Rev. A.*, **34**, 3373 (1986).
17. S. Zumer, *Phys. Rev. A*, **37**, 4006 (1988).
18. R. D. Sherman, *Phys. Rev. A*, **40**, 1591 (1989).

19. J. B. Whitehead, Jr., S. Zumer and J. W. Doane, *J. Appl. Phys.*, **73**, 1057 (1993).
20. J. Ding and Y. Yang, *Mol. Cryst. Liq. Cryst.* **238**, 47 (1994).
21. J. V. Champion, A. Killey and G. H. Meeten, *J. Polym. Sci. Polym. Phys. Ed.*, **23**, 1467 (1985).
22. G. H. Meeten, *J. Polym. Sci. Polym. Phys. Ed.*, **22**, 2159 (1984).
23. H. Zhang, F. Li and Y. Yang, *Chn. J. Funct. Polym.*, **4**, 265 (1991).
24. J. D. Margerum, A. M. Lacker, E. Ramos, K. C. Lim and W. H. Smith, Jr., *Liq. Cryst.*, **5**, 1477 (1989).
25. J. Ding, *M. A. Thesis* (Fudan University, 1991).
26. J. Ding and Y. Yang, *Jpn. J. Appl. Phys.* **33**, 1400 (1994).
27. J. Ding and Y. Yang , unpublished.
28. R. Ondris-Crawford, E. P. Boyko, B. G. Wagner, J. H. Erdmann, S. Zumer and J. W. Doane, *J. Appl. Phys.*, **69**, 6380 (1991).
29. A. Golemme, S. Zumer, J. W. Doane and M. E. Neubert, *Phys. Rev. A.*, **37**, 559 (1988).
30. J. Lu, F. Li and Y. Yang, *3rd National Sym. on Polym. Liq. Cryst.*, (Jinan, P. R. China, 1991).
31. N. A. Vaz and G. P. Montgomery, Jr., *J. Appl. Phys.*, **62**, 3161 (1987).
32. G. P. Montgomery, Jr. and N. A. Vaz, *Phys. Rev. A*, **40**, 6580 (1989).
33. G. P. Montgomery, Jr., *J. Appl. Phys.*, **69**, 1605 (1991).

APPENDIX A: Derivation of Equations (17)–(21)

By Jacobian transformation of the volume element, we have

$$d\Omega = \frac{3}{4\pi} V \sin\beta \cos\beta \sin^3\alpha \, d\beta \, d\alpha \, d\varphi \tag{A.1}$$

where V is the volume of the nematic droplet. Substituting Equations (11), (12) and (A.1) into Equation (3), the integral expressions for Hv and Vv scattered amplitues can be readily written as:

$$E(Hv) = -3KE_0 V \alpha_{12} \times (A_1 I_{20202} + A_2 I_{20211} + A_3 I_{11101} + A_4 I_{11110} + A_5 I_{02000}) \tag{A.2}$$

and

$$E(Vv) = 3KE_0 V \left\{ \alpha_{20} \frac{sinU - U\cos U}{U^3} + \alpha_{12}(B_1 I_{20202} + B_2 I_{11101} + B_3 I_{02000}) \right\} \tag{A.3}$$

where I_{abcde} is defined as:

$$I_{abcde} = \frac{1}{4\pi} \int_0^{2\pi} \int_0^{\pi} \int_0^{\pi/2} \frac{(\sin\beta)^{a+1} \cos\beta (\sin\alpha)^{b+3} (\cos\alpha)^c (\sin\varphi)^d (\cos\varphi)^e}{1 - \cos^2\beta \cos^2\alpha} \times e^{-ikr\cdot s} \, d\beta \, d\alpha \, d\varphi \tag{A.4}$$

The bipolar nematic droplet has a symmetry point at the center of droplet, hence the term $\exp(-ik\mathbf{r}\cdot\mathbf{s})$ in Equation (A.4) can be simplified into $\cos(k\mathbf{r}\cdot\mathbf{s})$. With Taylor expanding,

$$\cos(k\mathbf{r}\cdot\mathbf{s}) = \sum_{n=0}^{\infty} \frac{1}{(2n)!} (k\mathbf{r}\cdot\mathbf{s})^{2n} \tag{A.5}$$

and

$$\frac{1}{1-(\cos\beta\cos\alpha)^2} = 1 + (\cos\beta\cos\alpha)^2 + (\cos\beta\cos\alpha)^4 + \cdots = \sum_{m=0}^{\infty} (\cos\beta)^{2m}(\cos\alpha)^{2m} \tag{A.6}$$

Substituting Equations (7), (A.5) and (A.6) into Equations (A.2)–(A.4) and integrating term by term, the final expressions for SALS from a single bipolar nematic droplet can be obtained (see Equations (17)–(21) in Section 2.2).

APPENDIX B: Analytical Formulae under the Zeroth Order Approximation

Since the results of the zeroth order approximation for the index m can already reflect the main characteristics of the final scattering patterns, it is worthwhile to present corresponding analytical interpretations in the appendix:

$$E(Hv) = 3KE_0V\frac{\alpha_{12}}{(1-s_3^2)^3U^5}\left[H_{01}U^3\cos U + H_{02}U^2\sin U + H_{03}U\cos U + H_{04}\sin U + H_{05}U\cos(s_3U)\right] \tag{B.1}$$

where

$$H_{01} = (1-s_3^2)^2[A_1s_1^2s_3^2 + A_2s_1s_2s_3^2 + A_3s_1s_3(1-s_3^2) + A_4s_2s_3(1-s_3^2) + A_5(1-s_3^2)^2] \tag{B.2.1}$$

$$H_{02} = A_1s_3^2(1-s_3^2)^2 + (A_1s_1 + A_2s_2)s_1(1-12s_3^2+17s_3^4-6s_3^6) + 2(1-s_3^2)^3[-A_33s_1s_3 - A_43s_2s_3 + A_52(1-3s_3^2)] \tag{B.2.2}$$

$$H_{03} = -(H_{04} + H_{05}) \tag{B.2.3}$$

$$H_{04} = 15(1-s_3^2)^3(-A_2s_1s_2 + A_3s_1s_3 + A_4s_2s_3) \tag{B.2.4}$$

$$H_{05} = -A_12(1-s_3^2-4s_1^2) + A_28s_1s_2 \tag{B.2.5}$$

and

$$E(Vv) = 3KE_0V\left\{\alpha_{20}\frac{\sin U - U\cos U}{U^3} - \frac{\alpha_{12}}{(1-s_3^2)^3U^5} \times \left[V_{01}U^3\cos U + V_{02}U^2\sin U + V_{03}U\cos U + V_{04}\sin U + V_{05}U\cos(s_3U)\right]\right\} \tag{B.3}$$

where

$$V_{01} = (1 - s_3^2)^3 [B_1 s_1^2 s_3^2 + B_2 s_1 s_3 (1 - s_3^2) + B_3 (1 - s_3^2)^2] \tag{B.4.1}$$

$$V_{02} = B_1 (s_3^2 - 2s_3^4 + s_3^6 + s_1^2 - 12 s_1^2 s_3^2 + 17 s_1^2 s_3^4 - 6 s_1^2 s_3^6) - B_2 6 s_1 s_3 (1 - s_3^2)^3 + B_3 2 (1 - 3 s_3^2)(1 - s_3^2)^3 \tag{B.4.2}$$

$$V_{03} = -(V_{04} + V_{05}) \tag{B.4.3}$$

$$V_{04} = 3(1 - s_3^2)^3 (1 - 5 s_3^2 + B_2 5 s_1 s_3) \tag{B4.4}$$

$$V_{05} = -B_1 2 (1 - s_3^2 - 4 s_1^2) \tag{B.4.5}$$

in which the other variables are denoted in Section 2.